Experimental measurements of macro-particle dispersion in grid turbulence and application to a stochastic numerical model for solid body turbulent diffusion

A. Joly[1], F. Moulin[2], S. Cazin[2], A. Astruc[2] & D. Violeau[1]
[1]*Saint-Venant Laboratory for Hydraulics, Université Paris-Est, France*
[2]*Institut de Mécanique des Fluides de Toulouse, Université de Toulouse INPT, France*

Abstract

The transport of solid bodies (e.g. algae, debris or sediment grains) along a coastline is a necessary consideration for the sustainable management of beaches and coasts, including any structure built along the shoreline. The use of a stochastic transport model allows to take into consideration a wide scale of physical processes, such as the current around a coastal structure, the turbulence generated by the flow and the effects of inertia and drag of each body. In order to validate the developed model, in view of industrial applications, a set of experiments was performed. The objective of the experiments was to validate to numerical model in isotropic turbulence. The experiment consisted of oscillating grid generated turbulence, inside which spherical particles were released. Measurements were done using PIV to quantify the turbulence and video particle tracking to measure displacement. The experimental result were then compared to various numerical simulations.
Keywords: particle diffusion, stochastic transport, isotropic turbulence, oscillating grid, particle image velocimetry, video particle tracking.

WIT Transactions on Engineering Sciences, Vol 70, © 2011 WIT Press
www.witpress.com, ISSN 1743-3533 (on-line)
doi:10.2495/MPF110091

1 Introduction

The transport of solid bodies (e.g. algae, debris or sediment grains) is a reoccurring problem for many industrial structures built along the shore line interested in the sustainable management of said coast. Currently most numerical models of solid body behaviour along a shoreline focus on the growth and evolution of an population (or ensemble) of bodies. These models require large time scales (days–months) and are relevant for large-scale areas (10–100 km), for example see [1] or [2] for algal blooms (a population of solid bodies). But these models prove ineffective when designing civil engineering works necessary for the sustainable management of coastal industrial structures. These problems require smaller scales of investigation (10 m–1 km and 1–24 h) as the motion of a body will be affected by tides, waves, and diffusion due to turbulence (see [3]). The model presented in [4] develops a stochastic approach for predicting the trajectory of individual particles. To validate this model, a set of experiments were done. In the first instance particles were released in static water of different densities; this was done to test the settling body velocities, as well as validate the particle tracking protocol. Finally particles were released into semi-isotropic turbulence, created using a pair of oscillating grids. Turbulent properties were quantified using PIV and LDV 2D measurements, and particle displacement statistics were measured using video particle tracking.

2 The particle transport model

The numerical particle transport model used in this paper is a stochastic model. It is divided into three stages. First the instantaneous local (at the emplacement of the particle) fluid velocity components (U_i) are calculated, using a stochastic model developed by [5]. It is then used to solve for the body velocity components (V_i), using the momentum equation. These are then integrated to give the position of the body (X_i), which is assumed to be isotropic (e.g. spheres):

$$dU_i(t) = -\frac{1}{T}U_i dt + C_i dt + B dW_i(t) \tag{1a}$$

$$dV_i(t) = \check{M} dU_i + \frac{1}{\tau_{part}}\left(U_i - V_i\right) dt + \check{g}_i dt \tag{1b}$$

$$dX_i(t) = V_i dt \tag{1c}$$

Where $dW_i(t)$ represents a Wiener process; the other coefficients are defined by the following equations:

$$T = \frac{1}{\frac{1}{2} + \frac{3}{4}C_0}\frac{k}{\varepsilon} \tag{2a}$$

$$\tau_{part} = \frac{2\overline{m}}{\rho_f S C_D(\mathrm{Re})\left|U_i - V_i\right|} \tag{2b}$$

$$\overline{m} = m + M \tag{2c}$$

$$\check{M} = \frac{\rho_f \Omega + M}{\overline{m}} = \frac{\rho_f \Omega + M}{m + M} \tag{2d}$$

$$\check{g}_i = \frac{m - \rho_f \Omega}{\overline{m}} g_i \tag{2e}$$

$$C_i = -\frac{1}{\rho_f}\frac{\partial \overline{P}}{\partial x_i} - \frac{1}{T}\overline{U_i} \tag{2f}$$

$$B = \sqrt{C_0 \varepsilon} \tag{2g}$$

For which ρ_f is the fluid density, k is the turbulent kinetic energy, ε is its dissipation rate, $\overline{U_i}$ are the mean fluid velocity components, $\overline{P}$ is the mean fluid pressure, m is the mass of the body, M is the magnitude of the added mass tensor, equal to $\frac{1}{2}\rho\Omega$ for a sphere, S is the cross-sectional area of the body, Ω is the area of the body, g_i are the components of gravity acceleration, C_D drag coefficient (for a sphere [6] provides an empirical solution as a function of the Reynolds number $\mathrm{Re} = |U_i - V_i|\, D/\nu$), D is the sphere diameter, and finally $C_0 = 2.1$.

As can be seen from the coefficients in equation 1a this model requires characteristic flow variables ($\overline{P}$, $\overline{U_i}$, k and ε) to be input to solve for the instantaneous local fluid velocity. These values are usually solved using another numerical model. It should also be noted that the two characteristic time (T and τ_{part}) can vary greatly in time, space and from each other, making the resolution of equations 1 difficult (see [4]). Finally this model will be compared to two other numerical models: the model presented in [3], where the particles are transported using Brownian motion and none of the solid body dynamics are considered, and the model presented in [7] where the inertia of each particle is ignored. Focus will later be placed the impact of modeling solid body dynamics, and in particular inertia.

3 Settling velocities

This first experiment was undertaken as a mean of testing the particle tracking protocol, and to serve as a reference for particles released in semi-isotropic turbulence. To record the trajectories of the different settling particles, two cameras were placed perpendicular to each other, with a tank filled with water at their focus point. The tank was tall enough to ensure that particles reached their settling velocities before entering the cameras' field of vision. The effects of parallax were taken into account and calibrations were done before hand, allowing to compute the particle positions from pixels to millimeters.

$$\text{Camera 1}: \quad \frac{x(mm)}{x(pixels)} = \alpha_y y(mm) + \beta_x \quad \frac{z_1(mm)}{z_1(pixels)} = \alpha_y y(mm) + \beta_x \tag{3a}$$

Table 1: The diameters and densities of the Nylon Polyamide PA 6,6 particles released into the fluid.

Diameter D (mm)	Standard Deviation (%)	Mean body density ρ_s (kg/m^3)	Standard Deviation (%)
20	0.254	1129	0.0740
10	0.508	1128	0.301
5	1.02	1115	0.125
2	2.54	1062	2.42

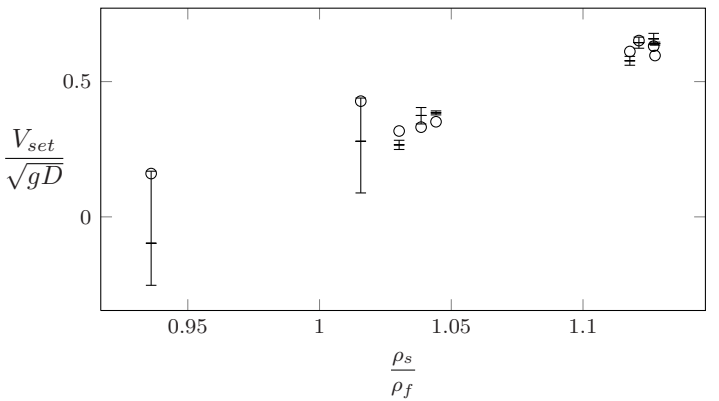

Figure 1: Dimensionless settling velocities against different particle fluid density ratios. "–" is the analytical solution (equation 4) plotted with its 95% confidence interval error bars and "○" are the experimental measurements.

$$\text{Camera 2}: \quad \frac{y(mm)}{y(pixels)} = \alpha_x x(mm) + \beta_y \quad \frac{z_2(mm)}{z_2(pixels)} = \alpha_x x(mm) + \beta_y \tag{3b}$$

The bodies used are spheres with diameters D and densities ρ_s, presented in table 1. They were released into two different fluid densities, $\rho_f = 1000$ and 1085 kg/m^3. Using equation (1b) it is possible to calculate the settling velocities of the bodies released in the fluid:

$$V_{set} = \frac{dX_z}{dt} = \frac{|m - \rho_f \Omega|}{(m - \rho_f \Omega)} \sqrt{\frac{2\,|m - \rho_f \Omega|}{\rho_f S C_D(\mathrm{Re})} g_z} \tag{4}$$

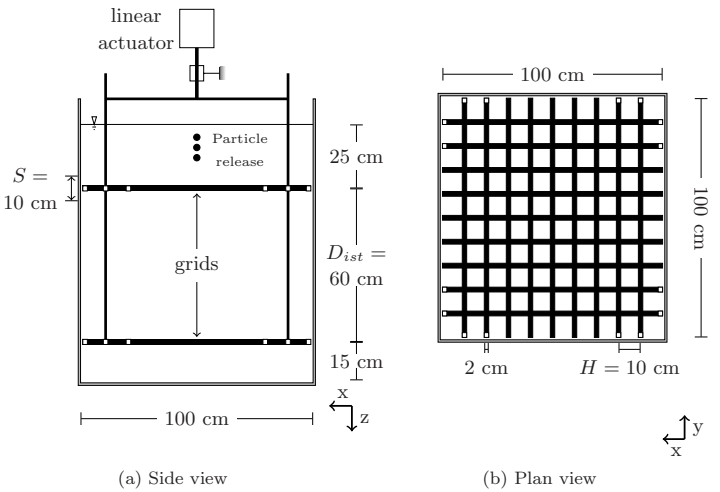

(a) Side view (b) Plan view

Figure 2: Dimensions for the turbulence generating system. The origin of the axis is located on the bottom right corner in the center of the lower grid.

Equation 4 is solved by iterations since Re depends on V_{set}. It should be noted that for this problem a rising velocity is assumed to be negative. The experimental values of V_{set} are then compared to the analytical results, for which the 95% confidence interval (calculated using the values in table 1) is presented in figure 1.

On figure 1 it is visible that the uncertainties are greater for low density ratios (ρ_s/ρ_f), but these correspond to the 2 mm diameter particles, for which the density had the greatest uncertainty (see table 1). In fact results show that for the smallest density ratio particles are settling, but the solution to the numerical model using the mean density gives a rising velocity. Nonetheless for large density ratios (with small particle densities uncertainties) the numerical model predicts the settling velocities accurately.

4 Turbulence quantification

The experimental device in figure 2 aimed to create near-isotropic turbulence by oscillating a pair of rectangular grids in a tank of still water. Several operating scenarios, in terms of oscillating of amplitudes (stroke S) and frequencies (f) were tested. The selected scenario, found to be most energetic, had a stroke of 10 cm and frequency of 1.67 Hz. The fluid velocities were then measured using Particle Image Velocimetry (PIV), in a 10×10 cm window of measurements located in between the two grids. Using these results the turbulent kinetic energy (k) and its rate of dissipation (ε) are estimated, see figure 3. Additional two-dimensional Laser Doppler Velocimetry (2D-LDV) was performed to validate the PIV measurements, and validate the horizontal isotropy.

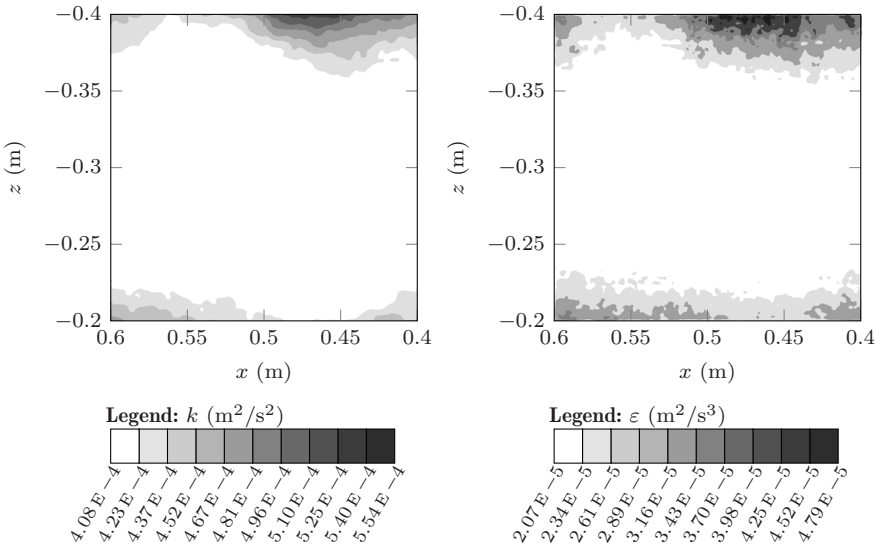

(a) Kinetic turbulent energy (k) (b) Turbulent energy dissipation rate (ε)

Figure 3: Turbulent quantification for double grid generated turbulence with an amplitude of 10 cm and frequency of 1.67 Hz.

Several papers give empirical formulae to model the turbulent characteristics of the flow resulting from a single oscillating grid (see [8–11]). Using these formulae, a crude hypothesis was stated; that the turbulent kinetic energy generated by each grid can be added. The semi-isotropic nature of the turbulence allows this assumption to give profile shapes for each turbulent characteristic in accordance to what can be expected. Constants were then adjusted to correspond to the constraints of the experiment. This gives the following equations:

$$\overline{U'_x} = \overline{U'_y} = \gamma_1 H^{\frac{1}{2}} S^{\frac{3}{2}} f \left[z^{-2} + (D_{ist} - z)^{-2} \right]^{\frac{1}{2}} \tag{5a}$$

$$\overline{U'_z} = \gamma_2 H^{\frac{1}{2}} S^{\frac{3}{2}} f \left[z^{-2} + (D_{ist} - z)^{-2} \right]^{\frac{1}{2}} \tag{5b}$$

$$k = \frac{1}{2} \left(2\gamma_1^2 + \gamma_2^2 \right) H S^3 f^2 \left[z^{-2} + (D_{ist} - z)^{-2} \right] \tag{5c}$$

$$\varepsilon = \frac{\gamma_3 \overline{U'_x}^3}{D_{ist}} \tag{5d}$$

Where H is the grid mesh size (10 cm), S is the stroke (10 cm), f is the frequency (1.67 Hz), D_{ist} is the distance between the two grids (60 cm), $\overline{U'_i}$ are the root mean square values of the velocity and γ_i are constants equal to 0.199, 0.252 and 5.05 respectively. 2D-LDV measurements have allowed to conclude

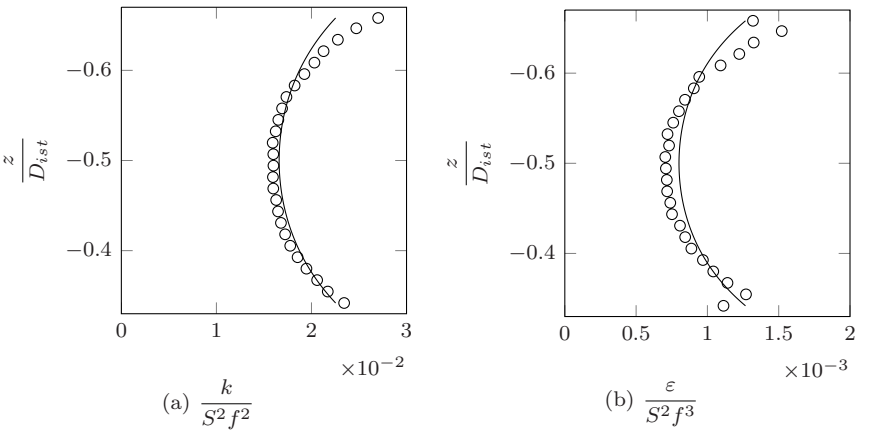

Figure 4: Vertical profiles for the turbulent kinetic energy and its dissipation. $S = 10$ cm and $f = 1.67$ Hz. "○" are the experimental values averaged along the horizontal axis and "——" is the empirical profile.

that $\overline{U_x'} = \overline{U_y'}$, but the constants γ_1 and γ_2 prove that the turbulence is not fully isotropic, but since their ratio is approximately 80%, the turbulence is semi-isotropic. In figure 4 the empirical and experimental profiles for the turbulent energy and its dissipation are plotted. These empirical values are in accordance with the measurements, and will therefore be used within the numerical model (equations 1 and 2) to calculate particle displacement statistics.

5 Particle displacement statistics

The particles described in table 1 were then released into the turbulence generated by the experimental setup presented in section 4, at location $(50, 50, 85)$ cm, for two different fluid densities, $\rho_f = 1000$ and 1084 kg/m^3. Three representative cases will be presented here: 20 mm particles in 1084 kg/m^3 fluid, 10 mm particles in 1000 kg/m^3 fluid and 5 mm particles in 1000 kg/m^3 fluid. Particle trajectories were recorded in a similar fashion to section 3. Statistics were then computed on the displacements over time of these particles (as the particle velocities were not measured). These statistics were also computed using the model presented in equations 1 and 2, for which the boundary conditions were provided by the empirical model in equations 5. Furthermore these numerical and experimental results where compared against two other numerical models; Brownian motion as described by [3] and an inertia free model presented by [7].

Figure 5 plots probability density functions for the horizontal and vertical displacements (X_{hor} and X_{vert}) of solid bodies in semi-isotropic turbulence. In this figure plots are associated with three characteristic numbers: N_r which is the number of experimental results, ρ_s/ρ_f which gives the density ratios and D/λ_l which shows the ratio of the particle diameter. The coefficient dt, which appears

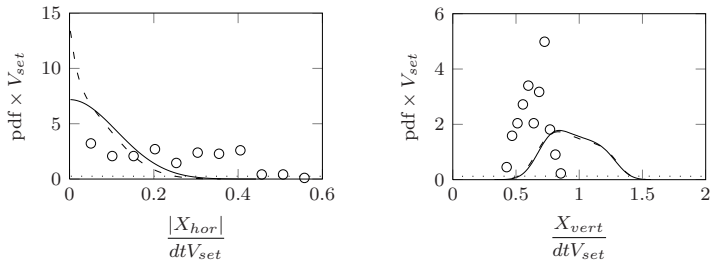

(a) $N_r = 105$, $\frac{\rho_s}{\rho_f} = 1.047$, $\frac{D}{\lambda_l} = 0.424$

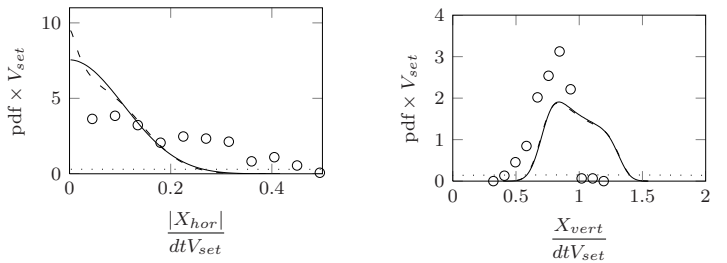

(b) $N_r = 178$, $\frac{\rho_s}{\rho_f} = 1.13$, $\frac{D}{\lambda_l} = 0.212$

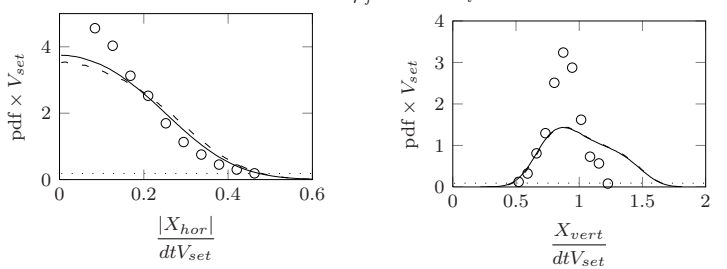

(c) $N_r = 354$, $\frac{\rho_s}{\rho_f} = 1.12$, $\frac{D}{\lambda_l} = 0.106$

Figure 5: Displacement statistics for bodies in grid turbulence of stroke 10 cm and a frequency of 1.67 Hz. "○" are the experimental values, "——" are the values for the numerical model (equations 1 and 2), "- - -" are the values for the numerical model if particle inertia was ignored [7] and "· · · ·" are the values for the numerical model for particles following Brownian motion [3].

in this figure, represents the time step, whereas the large eddy characteristic length (λ_l) is calculated using this equation : $\lambda_l = C_\mu^{3/4} k^{3/2}/\varepsilon$, with $C_\mu = 0.09$. This figure shows that the horizontal particle displacement statistics are driven by the turbulent diffusion, whereas the vertical displacement statistics are driven by the buoyant forces. Furthermore it should be noted that the numerical model present in this figure have a few uncertainties associated with their resolutions, the main

one being that particles are released above the window of measurement, and so the turbulent properties at the point of release haven't been validated. Nonetheless numerical results seem to be in accordance to the experimental results.

The first conclusion that can be derived from figure 5 is that a Brownian motion model (see [3]) is much too diffusive. [4] shows that the Brownian motion model would have been in accordance if the turbulence integral scale was much smaller. This implies that for turbulence of this magnitude, body properties (which are not considered in Brownian motion) have an impact on particle diffusion. The next conclusion is that for the largest particles (in figure 5(a)), the model from equations 1 and 2, seems to underestimate the horizontal diffusion, and overestimates the mean settling velocities. For smaller diameters (figures 5(b) and (c)) the model seems to give good results. When considering body properties ([4] and [7] models), it should be noted that particle inertia is most important in the cases where the particles are large and the density differences are small. For example, even though the model in equation 1 has difficulties sticking to the experimental results in figure 5(a), this model was developed under the assumption that the body was much smaller than the large scales of turbulence, adding inertial forces gives an improvement to just considering the drag forces (the model in [7]). These differences are less visible for the vertical displacement, where the displacement is driven by the buoyant forces. The assumption that the body was much smaller than the large scale of turbulence was done to keep the bodies passive; for the larger particles released in figure 5(a) it appears that its size cause it to affect the turbulence around it, requiring a more developed model such as Direct Numerical Simulations. When particles are smaller than the large scale of turbulence, but still of the same order (figure 5(b)), considering inertia gives an improvement, although considering the particle drag alone also gives a good estimate (the model in [7]).

6 Conclusion and further work

These experiments on the trajectories of solid bodies in semi-isotropic turbulence were undertaken to verify and observe the effect of solid body dynamics within an turbulent flow field. These experiment made it possible to conclude that the turbulent diffusion of these bodies is dependent on the forces acting upon it (see equation 1b). Therefore the first conclusion derived from these experiment is that a Brownian motion, which does not consider body properties, such as described in [3], might be limited when used in models developed to improve the sustainability of coastal structures. Furthermore considering the body's inertia gives an improvement to just considering drag forces (as was the case in [7]), but when these differences are most visible the particles' sizes will affect the turbulence around them, and results are only an approximation of the experimental results. Nonetheless for particle displacement statistics of smaller bodies, the model presented in this paper (equations 1 and 2) corresponds fairly well to the experimental results. It has therefore been shown that the model presented in [4] here can be

representative of the displacement of solid bodies in a turbulent flow, provided there is at least an order of magnitude between the large turbulent eddies characteristic size and the particle diameter. Future validating work will focus on validating this solid body diffusion model for a more physical flow regime, in view of being later applied to engineering problems. The next step will then be to repeat this methodology for a deceptively simple problem of an open channel flow around a groyne. Finally more complex geometries of real bodies, such as algae, will be taken into consideration.

References

[1] Salomonsen, J., Flindt, M., Geertz-Hansen, O. & Johansen, C., Modelling advective transport of Ulva lactuca (L) in the sheltered bay, Møllekrogen, Roskilde Fjord, Denmark. *Hydrobiologia*, **397**, pp. 241–252, 1999.

[2] Donaghay, P. & Osborn, T., Toward a theory of biological-physical control of harmful algal bloom dynamics and impacts. *American Society of Limnology and Oceanography*, **42**, pp. 1283–1296, 1997.

[3] Issa, R., Rougé, D., Benoit, M., Violeau, D. & Joly, A., Modelling algae transport in coastal area with the shallow water equations. *Journal of Hydro-Environment Research*, **3**, pp. 215–223, 2009.

[4] Joly, A., Violeau, D. & Minier, J., Modelling of the turbulent diffusion of algae in a coastal environment through a stochastic method with an exact integrator. *1st European IAHR congress*, Edinburgh, 4–6 May, 2010, 2010.

[5] Pope, S., *Turbulent Flows*. Cambridge University Press: Cambridge, 2000.

[6] Almedeij, J., Drag coefficient of flow around a sphere: Matching asymptotically the wide trend. *Powder Technology*, **186**, pp. 218–223, 2008.

[7] Peirano, E., Chibbaro, S., Pozorski, J. & Minier, J.P., Mean-field/PDF numerical approach for polydispersed turbulent two-phase flows. *Progress in Energy and Combustion Science*, **32**, pp. 315–371, 2006.

[8] De Silva, I.P.D. & Fernando, H.J.S., Oscillating grids as a source of nearly isotropic turbulence. *Physics of Fluids*, **6(7)**, pp. 2455–2464, 1994.

[9] Cheng, N.S. & Law, A.W.K., Measurements of turbulence generated by oscillating grid. *Journal of Hydraulic Engineering*, **127(3)**, pp. 201–208, 2001.

[10] Al-Homoud, A. & Hondzo, M., Energy dissipation estimates in oscillating grid setup: LDV and PIV measurements. *Environmental Fluid Mechanics*, **7**, pp. 143–158, 2007.

[11] Holzner, M., Liberzon, A., Guala, M., Tsinober, A. & Kinzelbach, W., Generalized detection of a turbulent front generated by an oscillating grid. *Experiments in Fluids*, **41**, pp. 711–719, 2006.